Int. J. Multiphase Flow, Vol. 2, pp. 35–49. Pergamon/Elsevier, 1975. Printed in Great Britain.

DOWNWARDS CO-CURRENT ANNULAR FLOW

D. R. WEBB† and G. F. HEWITT‡

†Department of Chemical Engineering, University of Manchester Institute of Science and Technology

and

‡Chemical Engineering Division, A.E.R.E., Harwell, Berks., England

(*Received* 1 *August* 1974)

Abstract · This paper summarizes a study of the characteristics of downwards annular two-phase flow. The measurements reported are of film thickness, wave velocity and frequency, local pressure fluctuations, pressure gradient and liquid entrainment. The most important new feature of the work is the use of continuous data recording with either on-line or off-line statistical analysis. Experiments were carried out with air–water flows in tubes of 3.18 and 3.82 cm bore. It is shown that the interfacial characteristics of the flow may require at least 5 m for full development at some flow rates and most measurements were carried out with an entrance region of this length. It is also shown that the pressure fluctuations, characteristic of this two-phase flow regime, are primarily due to pressure surges caused by disturbance waves in the system passing through the exit device. A new regime map is proposed, based on experimental evidence, in which several distinctive types of interfacial behaviour are noted.

1. INTRODUCTION

A great deal of work has been carried out on the experimental measurement of the interfacial characteristics and flow properties of annular upwards two-phase flow. Various studies of this type were reported by Hall Taylor *et al.* (1963) and Nedderman & Shearer (1963). More recently Hewitt (1969) summarized extensive work carried out on this subject by the U.K.A.E.A. at Harwell. In upwards flow, two characteristic regimes were observed. At high gas flow rates and low liquid flow rates the liquid surface is covered by relatively small waves ("ripples"), whereas for high liquid flow rates, much larger waves ("disturbance waves") are observed. The latter waves have amplitudes many times the mean film thickness and a characteristic circumferential continuity and persistence in flowing along the channel.

By comparison relatively little work has been done to study co-current downwards annular flow. The only previous comparable study is that of Telles (1968), who investigated co-current downwards flow in a rectangular duct. It is beyond the scope of the present paper to give complete details of all the data obtained in this study. However a series of reports have been issued by Webb (1971 a, b, c, d, e), which give complete details of the various measurements.

2. EXPERIMENTAL MEASUREMENTS

Experimental measurements made in this study were of film thickness, local pressure, pressure drop and liquid entrainment. Film thickness measurements were made in both the 3.18 cm and the 3.82 cm tubes, whereas pressure and liquid entrainment measurements were confined to the 3.82 cm tube.

(a) *Film thickness*

A conductance probe method was used for determining film thickness. To allow consistency with the work of Telles (1968), each probe consisted of two platinum foils cast in

an epoxy resin flange and machined flush with the inner diameter of the tube. The foils were 1.27 cm wide, 0.0254 cm thick and 0.508 cm apart in the direction of flow. Four such conductance probes were placed at equal intervals around the periphery of the tube at two down-stream locations, 5.48 m and 6.01 m respectively below the liquid inlet. This probe system was used for all film thickness measurements made in the 3.82 cm bore tube.

For the experiments relating to the effect of entrance length on the interfacial structure, alternative probes were used as described by Hewitt, King & Lovegrove (1962). These probes consisted of two circular stainless steel rods of 0.318 cm dia installed flush with the tube wall 1.27 cm apart in the direction of flow.

Both types of probe were calibrated by inserting machined plugs into the flow tube so as to form an annular gap. This gap was filled with a calibration fluid of known thickness and conductivity. By using a set of plugs, a calibration curve was established. Full details of the method of calibration for both probe geometries are given by Webb (1971 a, b).

An electronic circuit was developed to measure conductance. Briefly, an audio frequency signal was passed through the probes, the magnitude of the current depending on the admittance of the probe at the instantaneous value of the film thickness. This current also passed through a transformer in series with the probe. The resultant signal from the transformer, which was proportional to the instantaneous film thickness, was rectified. The audio frequency component was smoothed out and the signal amplified before passing to a recording system. The use of transformer coupling was desirable in eliminating interference between adjacent probes. In part of the work, a multitrack tape recorder or a high speed pen recorder was used to record the time varying film thickness. Alternatively the output from the film thickness probes could be fed directly to an on-line correlation device described in (3.2).

(b) *Local pressure fluctuations*

The instrumentation was so arranged that film thickness and pressure could be measured at the same location. A small hole was drilled between the electrodes of the conductance probes to convey liquid to the diaphragm of a pressure transducer, mounted in the tube wall. The mechanical design was such that the diaphragm was situated as close as possible to the falling liquid film in the tube (1.27 cm), and provision was included for bleeding the connecting channel, so that the system should have a high frequency response. These could be recorded on either output device or fed directly to the correlator.

(c) *Pressure drop*

Pressure gradient was measured by measuring the pressure drop between points at distances of 5.48 m and 6.01 m from the inlet. For these measurements a new type of manometer system was employed. This consisted of a sensitive differential pressure cell coupled with a water–carbon tetrachloride manometer, which corrected for the static head difference between the measurement points. Details of this manometer system are given by Webb (1971 c).

(d) *Liquid entrainment*

The liquid entrainment flow in the gas phase was determined at a position about 6 m below the liquid inlet. It was found that the porous sinter method, described by Hewitt *et al.* (1962), did not work effectively for downwards flow since the liquid tended to leak from the bottom of the sinter section. A slit device was developed (Webb 1971 c) which was similar to that originally used by Gill *et al.* (1965). The necessity of using the latter device most probably reduced the accuracy of the measurements, compared with those made in upwards flow.

All experiments in the 25 m long 3.18 cm tube were carried out with an outlet pressure of 204.9 kN/m^2, whereas the experiments in the 6 m long, 3.82 cm tube were carried out at an outlet pressure of 135.9 kN/m^2 (Roberts 1969; Webb 1971 a, b). Potassium nitrate was added to the circulating water in both sets of experiments to increase the liquid film conductivity. Liquid rates used were in the range 36–455 kg/hr and gas rates were in the range 0–182 kg/hr.

3. ANALYSIS

The analysis can be divided into two main types: non-statistical and statistical. The non-statistical measurements were of overall average parameters like pressure gradient and liquid entrainment, the determination of the onset of disturbance waves, manual and mechanical measurements of wave frequency and manual measurements of wave velocity. The statistical methods employed included analogue computer methods for the determination of the amplitude distribution of film thickness and the power spectral density, and finally, the use of correlation analysis with an on-line computing device. It is convenient to discuss the various techniques under the headings of the parameters measured.

3.1 *Wave frequency*

The measurements were concentrated mainly in the region of disturbance waves, using three methods:

(a) *Manual counting.* This involves the examination of chart recorder outputs of the type illustrated in figure 1 to assess which of the waves fall into the "disturbance wave" category, and to count the number in a given length of trace. From this, the wave frequency can be determined. Unfortunately, the direct counting from traces is reliable only when the disturbance waves are well defined. In an attempt to overcome this difficulty, a mechanical counting method was devised.

(b) *Mechanical counting.* With this technique, a count was obtained of the number of times the film thickness trace passed above a set level. The film thickness record from the tape recorder was fed into an analogue computer circuit, linked to a bank of mechanical counters (Webb 1971 e). Figure 2 shows a typical set of results of the frequency at which the film thickness passed above various set levels, plotted on the abscissa. The various curves are for different liquid rates with gas rate constant. The well defined plateau region, where wave count is independent of film thickness, indicates few wave peaks in this band. The waves are well defined and the frequency is readily obtained. However this form of result was not always obtained and it is often difficult to estimate wave frequency by this method.

(c) *Power spectral density determination.* The objective of a power spectral density analysis was to remove the subjectivity inherent in frequency determination by the fore-

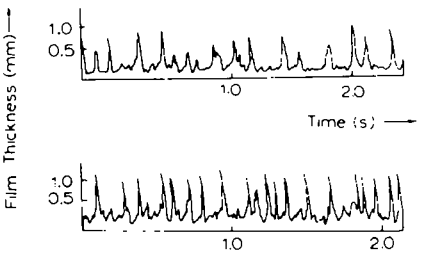

Figure 1. Typical chart recorder outputs. Upper trace: gas rate 45.5 kg/hr, liquid rate 90.1 kg/hr. Lower trace: gas rate 159.1 kg/hr, liquid rate 90.1 kg/hr.

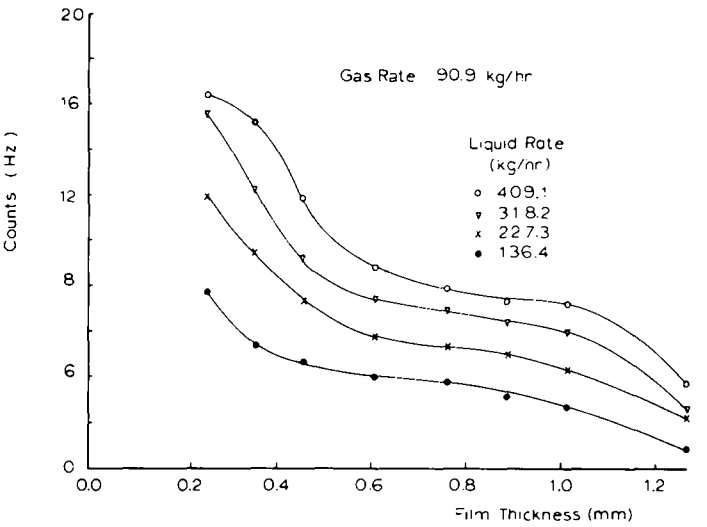

Figure 2. Frequency of film thickness crossing set levels.

going two methods. An analogue computer circuit was set up (Webb 1971 e), which converted the voltage output from the conductance probes, as recorded on the tape recorder, into a voltage which was proportional to the instantaneous film thickness. Secondly it filtered this signal to identify the relative power in any given frequency band. The approximate band width of the filter was 0.25 of the centre frequency. Typical results obtained by this method are illustrated in figures 3 and 4.

Comparisons between the various methods indicated that the peak frequency obtained from figure 3 corresponded quite closely to the values estimated by the other methods, though in general, it was somewhat lower. Figure 5 shows frequency data obtained by the counting method with wave frequency as a function of gas rate with liquid rate as a parameter. There are essentially two regions, one in which gas rate has a small or zero effect on wave frequency and one in which the wave frequency rises approximately linearly with increasing gas rate.

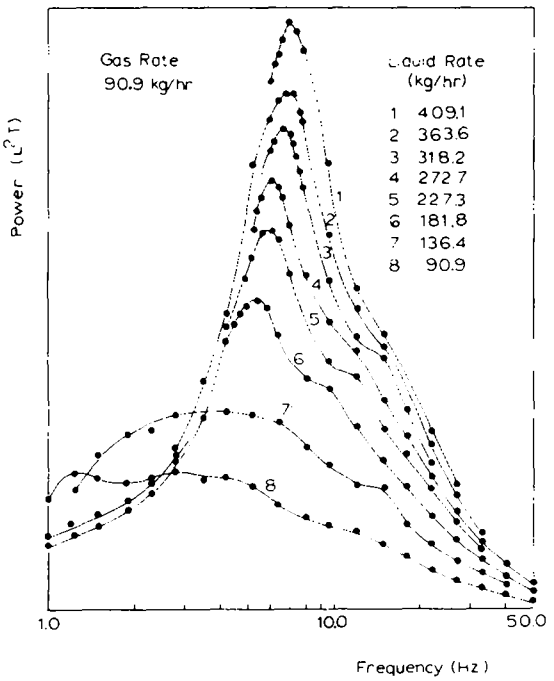

Figure 3. Power spectral density functions of film thickness.

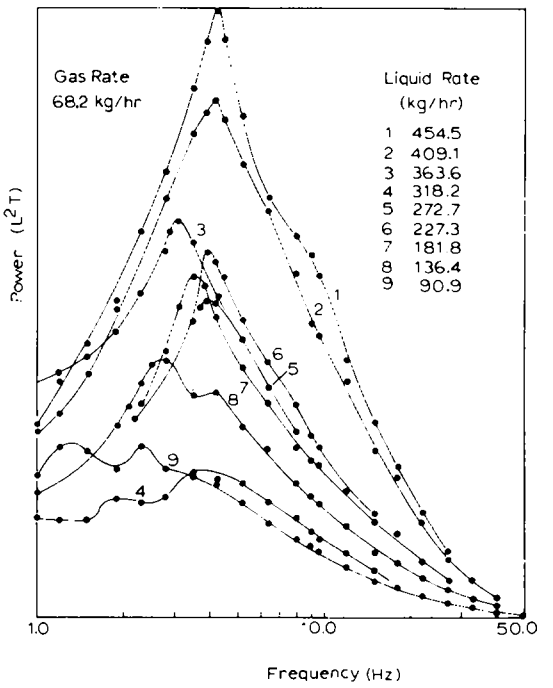

Figure 4. Power spectral density functions of film thickness.

3.2 *Wave velocity*

Two methods were used for the measurement of wave velocities.

(a) *Direct measurement on pen recorder traces.* Pen recorder traces were obtained of film thickness, measured simultaneously at positions displaced from one another along the tube. The individual waves were identified on the respective traces. For a given wave, the velocity was estimated from the time of passage between the two locations. The standard deviation of wave velocity was quite small: typically 0.15 m/sec for an average velocity of 2–3 m/sec. Thus, the determination of velocity from pen recorder traces is more successful than that of frequency. However, when the disturbance waves are difficult to identify on a trace, there still remains a strong element of subjectivity.

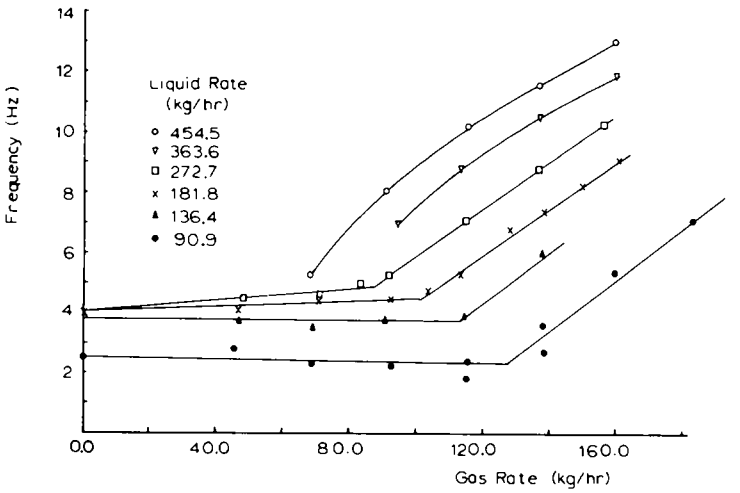

Figure 5. Counted wave frequency.

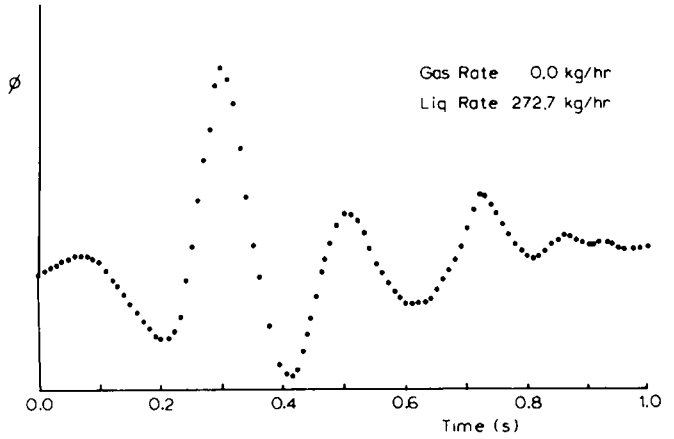

Figure 6. Cross-correlogram of film thickness.

(b) *Estimation from correlation analysis.* The wave velocity may also be determined using the technique of cross-correlation. The following function ϕ is determined.

$$\phi(\tau) = \frac{1}{T}\int_0^T f(t)g(t-\tau)\,dt$$

where $\phi(\tau)$ is the cross correlation function of $f(t)$ and $g(t)$, T the averaging time and τ the time delay.

In the present experiments ϕ was determined as a function of the displacement time τ using a commercial correlator which produced simultaneously 100 discrete values of ϕ at equally spaced time intervals. This correlogram was displayed on an oscilloscope and figure 6 shows a typical output. The sharp peak in the output represents the time of passage of the disturbance waves between the measurement locations. From this displacement and the distance between probes the velocity of the waves can be determined (figure 7). There is a general increase in wave velocity with increasing liquid rate. The wave velocity usually increases with gas rate, though the behaviour at low gas rates is complex. In this region, the curves exhibit points of inflection which are related to the regime transitions discussed in section 5 below. The methods of measurement of wave velocity mentioned above agree quite well with one another at high liquid flows, though there is some small dis-

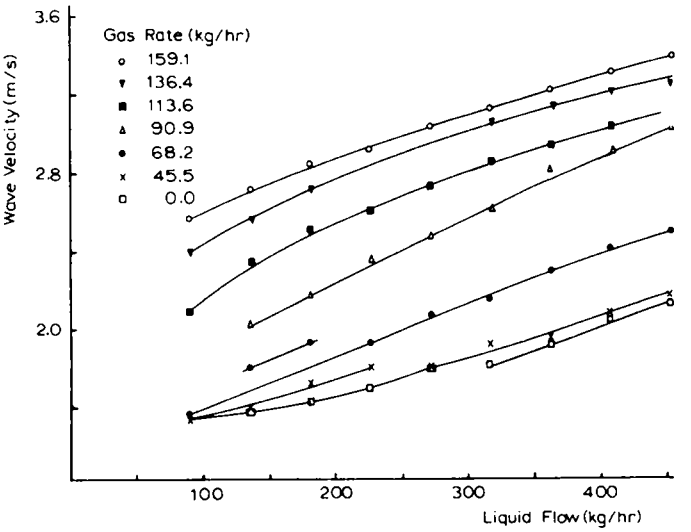

Figure 7. Wave velocity.

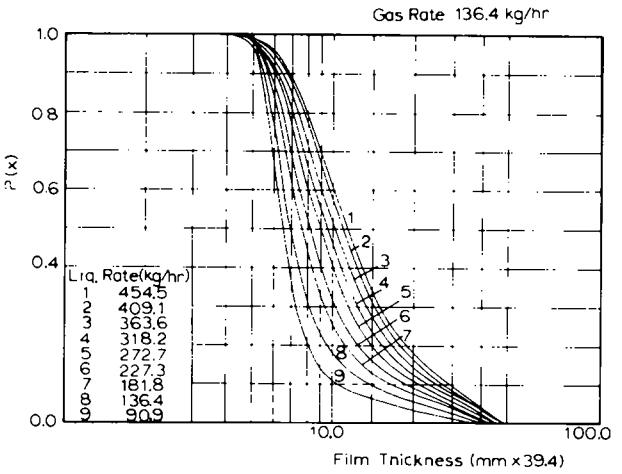

Figure 8. Amplitude distribution of film thickness.

crepancy at low liquid flow rates, where it may be difficult to identify unequivocally the infrequent disturbance waves on the pen recordings.

3.3 *Film thickness*

An amplitude distribution analysis was carried out on the tape records of film thickness for a wide range of gas and liquid rates. The voltage record was fed to an analogue computer, which was programmed to activate a switch when the voltage level exceeded a set value. When the switch was in the on position, current was fed to an integrator. Thus it was possible to measure the fraction of the time the signal remained above the set value. By adjusting this reference value the probability distribution function of the film thickness, $P(x)$, could be obtained.

Typical curves are shown in figure 8. At gas rates above 90.0 kg/hr the curves were of the regular form shown in figure 8, with $P(x)$ increasing with increasing liquid flow rate. For lower gas flow rates (e.g. figure 9) the behaviour was more complex. Again, these various types of behaviour are related to the regime description given in section 5.

The probability plots were integrated to give the mean film thickness. Extensive results are reported by Webb (1971 c). Figure 10 shows a comparison of the mean film thickness for the experiments on the 3.18 cm tube and the 3.82 cm tube. Agreement between the two sets of data is good, particularly in view of the fact that different types of probe geometry were used. Also shown in figure 10 are the results of Telles (1968) for a rectangular channel,

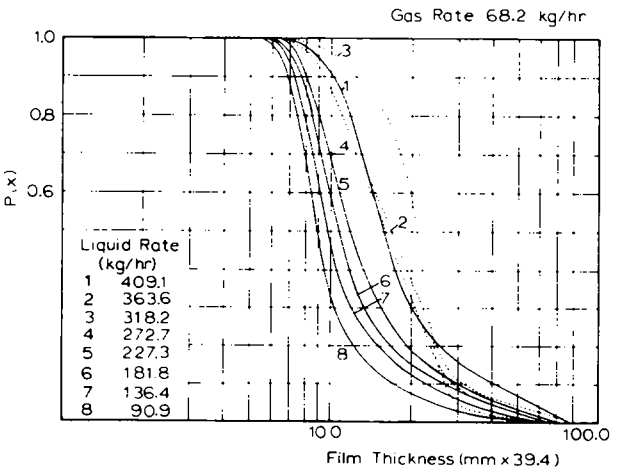

Figure 9. Amplitude distribution of film thickness.

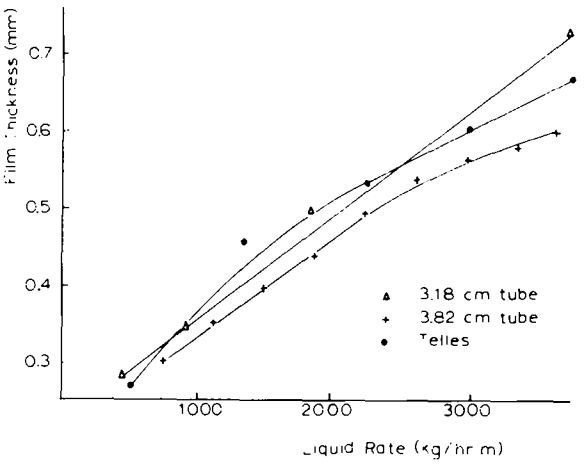

Figure 10. Comparison of mean film thickness.

showing a reasonable agreement with the present work. Some of the slight discrepancy may be due to unknown liquid distribution factors in Telles' experiments or to the effect of wall curvature.

3.4 *The relationship between film thickness variation and pressure fluctuations*

Fluctuations in local pressure are characteristic of two-phase flow systems. An attempt was made in the present work to relate these fluctuations to the passage of disturbance waves past a given point. When pressure fluctuations and film thickness were recorded simultaneously, it was noticed that relatively large perturbations in pressure occurred at about the same frequency as that of the disturbance waves, However, there appeared to be no relationship between the local variation in pressure and the local variation in film thickness. On further examination of the data, it was realized that the pressure fluctuations were considerably delayed from the film thickness fluctuations caused by the disturbance waves. This led to an investigation of the relationship between pressure fluctuation and film thickness fluctuation by the use of the cross-correlation technique mentioned above. A typical correlogram between pressure fluctuation and film thickness fluctuation is given in figure 11. A strong cross-correlation is observed with a peak at a given time delay. This time delay corresponded exactly to the time of passage of the wave from the measurement point to the tube exit. Thus the major pressure fluctuations in this type of system are likely to be caused by the interaction of the waves with the outlet, which in this case was a 90° elbow.

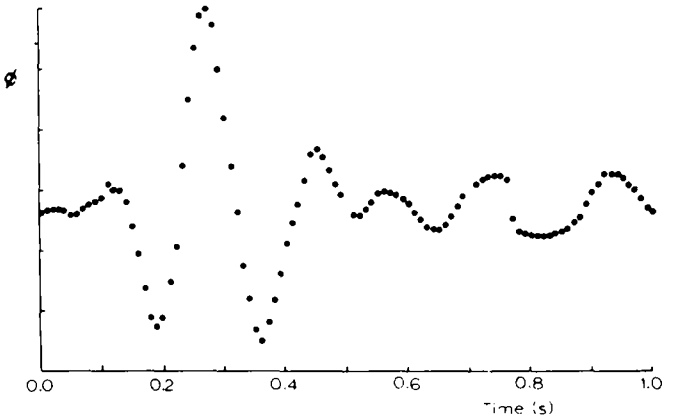

Figure 11. Cross-correlogram of local pressure and film thickness.

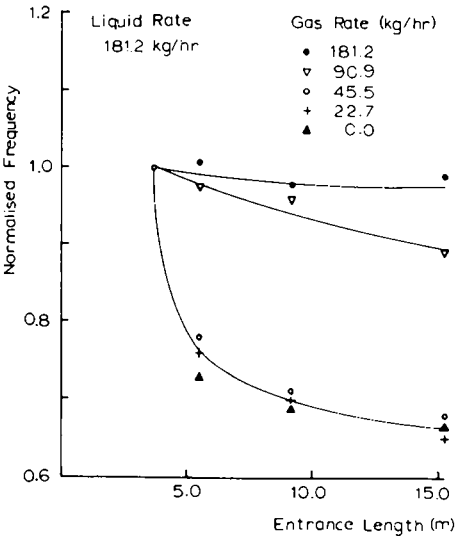

Figure 12. Effect of entrance length on wave frequency. (Wave frequency normalized by frequency at 3.66 m.)

It was thought that these pressure surges might influence interfacial conditions by affecting the process of wave formation and growth. This point was investigated by changing the exit geometry. A porous wall section was used to withdraw the liquid flow. This change reduced the magnitude of the largest fluctuations by a factor of five. However, no appreciable change in any of the measured variables was detected and it was concluded that the process of wave formation was independent of pressure surges set up in this manner.

4. THE EFFECT OF TUBE LENGTH

Experiments to determine the effect of tube entrance length on the interfacial characteristics were carried out in the 3.18 cm bore tube. Measurements were made at distances of 2, 4, 6, 8 and 15 m from the liquid inlet which was of the porous wall type. The variables most sensitive to changes of entrance length were the wave frequency and the amplitude distribution of film thickness (figures 12 and 13). Wave frequency decreases near the inlet but settles to a more or less constant value from 6 m onwards. Similar results are exhibited by the film thickness distributions which are coincident beyond 6 m. These data were for zero gas flow. For high gas flow rates there were some small changes even after 6 m but

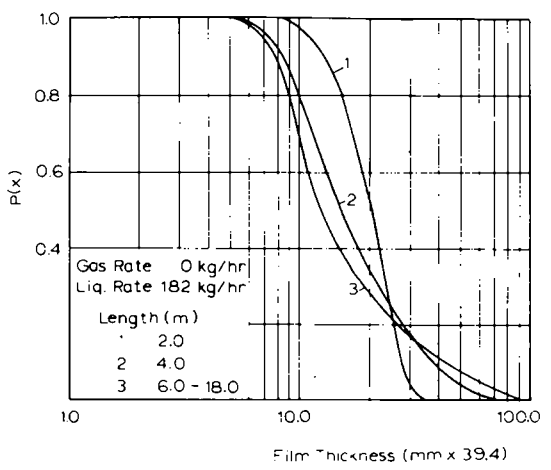

Figure 13. Effect of length on amplitude distribution of film thickness.

these are likely to be due to the expansion of the gas in the tube under the prevailing pressure gradient.

5. THE REGIMES OF INTERFACIAL BEHAVIOUR

On the basis of the present experimental observations, we propose a regime map for downward co-current flow as illustrated in figure 14. Four regimes are distinguished: ripple, regular disturbance wave, dual wave and thick ripple. The line ABC on figure 14 represents the transition from ripple wave structure to disturbance wave structure and is similar to that for upwards flow, though more complex in shape. The region AB shows a sharp transition of the type observed in upwards flow, but the region BC is less well defined: the experiments on determination of this transition line are described in detail by Webb (1971c). Line BD represents a transition between two regimes of disturbance wave behaviour. This transition is most clearly seen in figure 5 where wave frequency is almost constant at low gas flow rates but increases rapidly with gas flow rate above some threshold value. Line BD is the locus of the transition flow rates determined from figure 5. Thus we distinguish two regimes of disturbance waves: the first "regular disturbance wave" is similar to that observed in upwards flow. In this wave region, the waves are well defined and only one type of disturbance wave is observed. In the regular wave regime, the gas velocity is usually high and therefore the situation is controlled by the gas liquid interaction. In the "dual wave" region, on the other hand, the gas–liquid interaction is less important and the evidence seems to suggest that two basically different disturbance wave types coexist. The first type of wave occurs at zero gas velocity where a single peak is observed in the power spectral density and cross-correlation function measurements. As the gas velocity is increased from zero, at any given liquid rate within the dual wave regime, a second peak appears in the power spectral density and cross-correlation, and becomes more and more dominant as one passes from zero gas velocity up to the line BE. Conversely, the zero gas velocity type wave becomes less and less important as one increases the gas velocity towards line BE. Line BE represents the disappearance of the latter type of wave. The dual wave region is therefore characterized by the coexistence of two distinct types of waves. On passing over the boundary EF, a new region is entered where the increase in wave activity on the interface with increasing liquid flow rate (as observed in the dual wave region) is reversed and the wave activity falls. Finally, with further increases

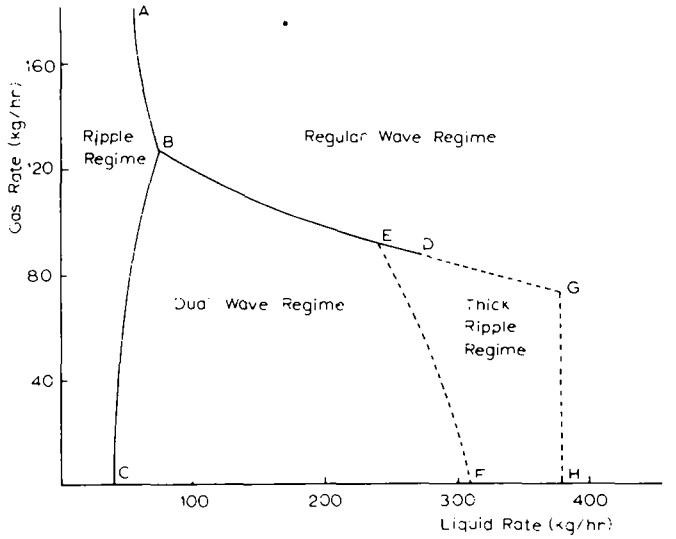

Figure 14. Regime map.

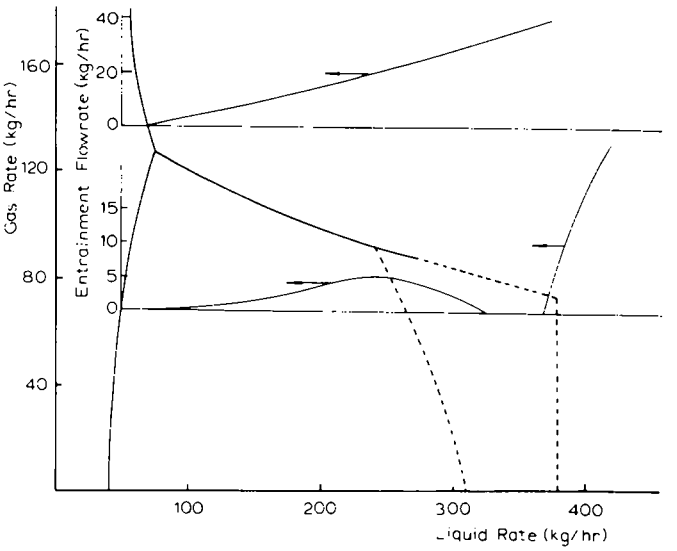

Figure 15. Entrained liquid flowrate.

of liquid rate at a given gas rate, the disturbance wave type of activity is returned. The transition into this regular disturbance wave region is tentatively given by line GH, though we do not have very much information in the region of liquid flow rates beyond this line.

The inter-relation of the two-phase flow parameters with these regime transitions can now be described by considering each of the parameters in turn as follows:

(1) *Liquid entrainment*

Figure 15 shows the behaviour of liquid entrainment with increasing liquid rate at two distinct gas rates, superimposed on the regime diagram. At 136 kg/hr gas flow rate, liquid entrainment begins at the transition from the ripple wave to the disturbance wave region and increases monotonically with increasing liquid flow. On the other hand, at a gas flow rate of 68 kg/hr there is a more complex change in entrainment flow rate with liquid flow rate. In particular the fall in wave activity through the "thick ripple" region is accompanied by a decrease in entrainment flow rate. Further detailed data are given by Webb (1971c).

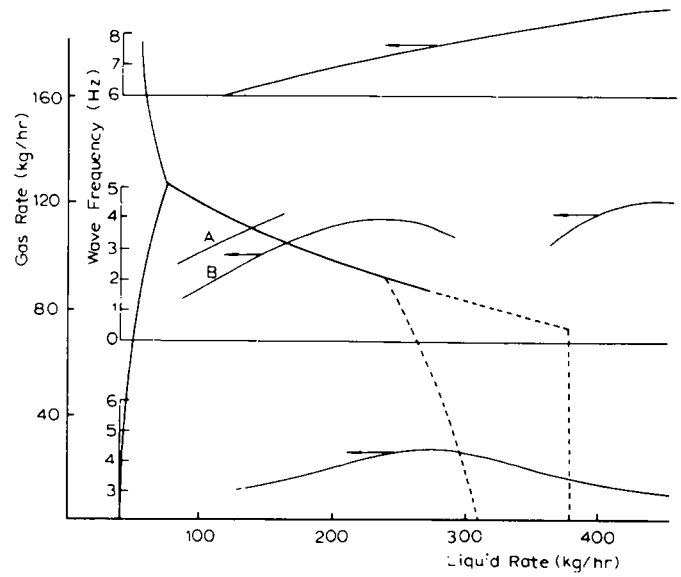

Figure 16. Wave frequency.

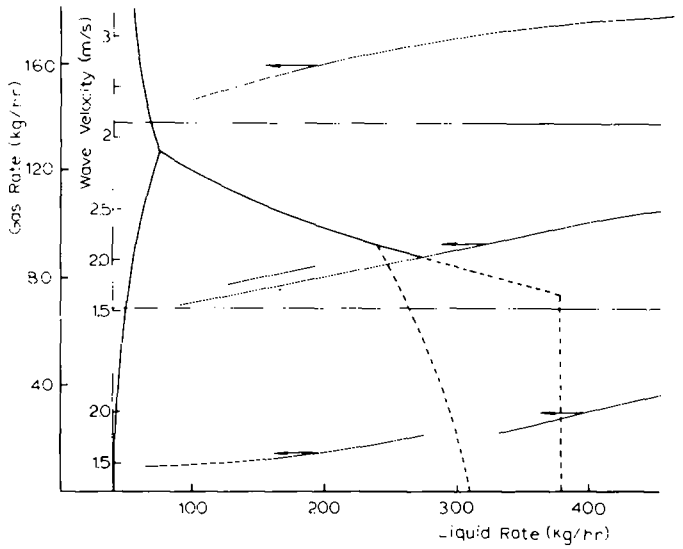

Figure 17. Wave velocity.

(2) *Wave frequency*

Figure 16 shows the data for wave frequency plotted on the regime map. At a gas rate of 159 kg/hr, the disturbance wave frequency increases monotonically with increasing liquid rate from the point of onset of disturbance waves. At a gas rate of 68 kg/hr, there is a complex variation in wave frequency as one passes successively through the dual wave, thick ripple and regular disturbance wave regions. At zero gas velocity, the wave frequency increases with increasing liquid rate up to the transition to the thick ripple region and then shows the reverse trend. In figure 16, we distinguish between waves of the high gas velocity type (type A) and those of the zero gas velocity type (type B).

(3) *Disturbance wave velocity*

The results for disturbance wave velocity are shown in figure 17 relative to the regime map. At a gas rate of 136 kg/hr, the velocity increases monotonically with increasing liquid rate. At a gas rate of 68 kg/hr, two characteristic velocities are observed in the dual wave region, and the velocity passes through a point of inflection as the transition to the thick ripple region is approached. A similar pattern (though with only one type of wave observed) is seen at zero gas velocity.

(4) *Liquid film thickness*

Measurements of film thickness were presented in the form of the probability distribution function $P(x)$. The distribution function and hence the film thickness can be characterized by the moments, M_n, of $P(x)$ about the origin:

$$M_n = \int_0^x x^n P(x)\,dx.$$

The zeroth moment is the mean film thickness whereas the first and second moments increasingly reflect the importance of the wave structure, and show distinctive behaviour in the various regimes of figure 14. The most dramatic effect is shown by the second moment where the effect of the wave structure is strongly felt (figure 18). At a gas flow rate of 136 kg/hr there is a regular increase in M_2 with increasing liquid flow rate. However at 68 kg/hr the reduced importance of the wave structure in the thick ripple regime is very clearly shown. Plotted on the same diagram is the mean film thickness at 68 kg/hr. It is clearly seen that

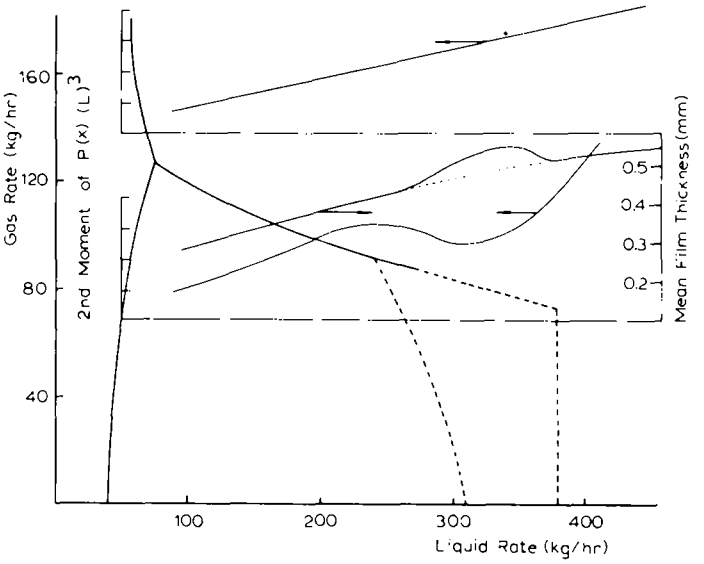

Figure 18. Moments of amplitude distribution of film thickness.

the decrease in wave character is accompanied by an increase in substrate film thickness. The decrease in wave importance means a lower interfacial roughness and consequently a lower interfacial shear stress. For a given liquid flow rate therefore the film thickness must be increased. As the end of the thick ripple region is approached, the wave structure is reinstated with an increase in the interfacial shear stress and a *decreasing* film thickness with increasing liquid flow rate. This decrease in interfacial shear stress is confirmed by the pressure drop data which also show a reverse trend of decreasing pressure drop with increasing liquid flow rate in this region (Webb 1971c).

(5) *Statistical variables*

The power spectral density function, the amplitude distribution of film thickness and the cross-correlation function all show characteristic features in the various regimes. The amplitude distribution of film thickness (figure 9) for a gas flow rate below the transition to the regular wave regime shows the decrease in wave character as the thick ripple zone is traversed and the re-establishment of wave dominance at the higher flow rates. Contrast the perfectly regular behaviour of the film thickness distribution at a gas rate above the transition (figure 8). The power spectral density function shows the most dramatic changes as one traverses the various low gas flow rate regimes (figure 4). Notice the successive development of twin peaks in the function, the elimination of one of these peaks, the rapid drop in power through the thick ripple regime and the subsequent re-establishment of wave conditions as liquid flow rate is increased. This is in marked contrast to the behaviour in the regular wave regime (figure 3). The cross-correlation function of wave velocity showed corresponding behaviour at low gas flow rates, a double peak developing in the dual wave regime (Webb 1971e).

6. CONCLUSION

Extensive data have been obtained on downwards co-current annular flow. The most important observations made from this data are that there exist various regions of interfacial behaviour in downwards co-current flow depending on the gas and liquid rates used. All the important parameters of this type of two-phase flow are affected directly or indirectly by the existence of these regions.

Acknowledgement—The authors wish to acknowledge assistance by Mr. D. Benn, AERE, Harwell in setting up the electronic circuitry and also gratefully acknowledge many useful discussions with Professor A. E. Dukler (University of Houston) who was on sabbatical leave at Harwell when this work was in progress.

REFERENCES

GILL, L. E., HEWITT, G. F. & LACEY, P. M. C. 1965 Data on the upwards annular flow of air–water mixtures. *Chem. Engng Sci.* **20**, 71–88.

HALL TAYLOR, N. S., HEWITT, G. G. & LACEY, P. M. C. 1963 The motion and frequency of the large disturbance waves in annular two-phase flow of air–water mixtures. *Chem. Engng Sci.* **18**, 537–552.

HEWITT, G. F. 1969 Disturbance waves in annular two-phase flow. *Proceedings of the Symposium on Two-Phase Flow Systems*, Leeds, September, Paper No. 18, p. 144. Institution of Mechanical Engineers, London.

HEWITT, G. F., KING, R. D. & LOVEGROVE, P. C. 1962 Techniques for liquid flow film and pressure drop studies in annular two-phase flow. AERE—R.3921.

NEDDERMAN, R. M. & SHEARER, C. J. 1963 The motion and frequency of large disturbance waves in annular two-phase flow of air–water mixtures. *Chem. Engng Sci.* **18**, 661–670.

ROBERTS, D. N. 1969 The Lotus (LOng TUbe System) air–water loop. Design and description. AERE—M.2175.

TELLES, A. C. DA S. 1968 Liquid film characteristics in vertical two-phase flow. Ph.D. Thesis, University of Houston.

WEBB, D. R. 1971a A study of the characteristics of downward annular two-phase flow, Part I: The effect of length. AERE—R. 6426.

WEBB, D. R. 1971b A study of the characteristics of downward annular two-phase flow, Part II: Description of experimental apparatus and its calibration. AERE—R.6426.

WEBB, D. R. 1971c A study of the characteristics of downward annular two-phase flow, Part III: Measurements of entrainment rate, pressure gradient, probability distribution of film thickness and disturbance wave inception. AERE—R.6426.

WEBB, D. R. 1971d A study of the characteristics of downward annular two-phase flow, Part IV: Pressure fluctuations. AERE—R.6426.

WEBB, D. R. 1971e A study of the characteristics of downward annular two-phase flow. Part V: Statistical measurements of wave properties. AERE—R.6426.

Résumé—Cet article résume une étude des caractéristiques des écoulements diphasiques annulaires descendants. Les mesures dont il est rendu compte concernent l'épaisseur du film, la vitesse et la fréquence des ondes, les fluctuations de pression locale, le gradient de pression et l'entrainement de liquide. La particularité nouvelle la plus importante de l'étude est l'utilisation d'enregistrements en continu des mesures, avec analyse statistique en temps réel ou différé. Les essais ont été menés avec des écoulements eau-air dans des tubes de 3,18 et 3,82 cm de diamètre intérieur. On montre que les caractéristiques interfaciales de l'écoulement peuvent nécessiter au minimum 5 m pour être pleinement établies, pour certains débits. La plupart des mesures ont été effectuées avec une région d'entrée de cette longueur. On montre également que les fluctuations de pression, caractéristiques de ces régime d'écoulement diphasique, sont dues principalement aux à-coups de pression causés par le passage des ondes de perturbation au travers du dispositif de sortie. On propose une nouvelle carte des régimes d'écoulement, basée sur des constatations expérimentales, et sur laquelle plusieurs types distincts de comportement interfacial sont indiqués.

Auszug—Dieser Artikel fasst eine Studie der Charakteristiken der Abwaertsstroemung zweier Phasen im Ringspalt zusammen. Ueber Messungen der folgenden Parameter wird berichtet: Schichtdicke, Wellengeschwindigkeit und -frequenz, oertliche Druckschwankungen, Druckgradient und Fluessigkeitsmitreissen. Die wichtigste neue Besonderheit dieser Arbeit ist die Anwendung kontinuierlicher Datenaufzeichnung, mit mitlaufender oder getrennt durchgefuehrter statistischer Analyse. Die Versuche wurden mit Luft-Wasser-Stroemung in Rohren von 3,18 und 3,82 cm Durchmesser durchgefuehrt. Es wird gezeigt, dass die Phasengrenzschicht-Charakteristiken der Stroemung bei manchen Geschwindigkeiten mindestens 5 m bis zur vollen Entwicklung

brauchen, und die meisten Messungen wurden mit dieser Einlaufslaenge gemacht. Ebenso wird gezeigt, dass die fuer diese Form der Zweiphasenstroemung charakteristischen Druckschwankungen vor allem durch Druckspruenge entstehen, die im System durch Stoerwellen beim Durchfluss durch die Austrittsvorrichtung verursacht werden, Es wird eine neue, auf Versuchsdaten beruhende Karte der Stroemungsformen vorgeschlagen, in der mehrere deutlich unterscheidbare Typen des Phasengrenzschicht-Verhaltens eingetragen sind.

Резюме—Настоящая работа подводит итоги изучения характеристик восходящего кольцеобразного двуфазного течения. Описаны измерения толщины нленки, скорости и частоты волны, местных колебаний давления, градиента давления и увлечения жидкрсти. Важнейшим новшеством данной работы является использование непрерывной записи показаний со статистическим анализом как входной линии, так и выходной. Были выполнены эксперименты с водо—воздушным потоком в трубах диаметром 3,18 и 3,82 см в свету. Показано, что межповерхностные характеристики такого нотока требуют при некоторых скоростях потока по крайней мере 5 м для своего полного развития, и большая часть экспериментов была выполнена при наличик входиой области такой длины. Показано также, что колебания давления, характеристики режима двуфазного течения обусловлены преимущественно ударными волнами давления, возбуждаемыми волнами возмущений в системе, проходящими через выходное устройство. Предложен новай карта распределения режимов, основанная на опытных данных, в которой отмечено несколько особенных типов иоведения на поверхности раздела.